

Isolated Ti in Si: Deep level transient spectroscopy, minority carrier transient spectroscopy, and high-resolution Laplace deep level transient spectroscopy studies

L. Scheffler, Vl. Kolkovsky,^{a)} and J. Weber

Technische Universität Dresden, 01062 Dresden, Germany

(Received 9 December 2014; accepted 16 January 2015; published online 30 January 2015)

Combining deep level transient spectroscopy (DLTS), high-resolution Laplace DLTS, and minority carrier transient spectroscopy studies, we question the identification of the dominant Ti-related defects introducing deep levels (E40, E150, and H180) in *n*- and *p*-type Si. The observed results cannot unambiguously support the models previously reported for these defects. The presence of the Poole-Frenkel effect describing the enhancement of the emission rates of E40 as a function of electric field is not consistent with the previous assignment of this defect to the single acceptor, whereas the absence of the enhancement of the emission rate of E150 under different reverse bias applied to the diode does not confirm the previous attribution of this defect to the single donor in *n*-type Si. The attribution of H180 to the double donor is in good agreement with our results. In contrast, the identical depth profiles obtained for E40 and E150 in bulk of as-grown, hydrogenated and annealed samples cannot be explained by the assignment of these levels to different defects.

© 2015 AIP Publishing LLC. [<http://dx.doi.org/10.1063/1.4906855>]

INTRODUCTION

Titanium is known as a transition metal (TM), which even in low concentrations can cause degradation of solar cell efficiency by as much as 50%.^{1,2} This is mainly believed due to the presence of deep Ti-related defects, which anneal out at very high temperatures (more than 900 °C). However, the charge state of these defects and their origin have become a subject of debates until now.^{3–8} Deep level transient spectroscopy (DLTS) measurements reveal three Ti-related peaks in both *n*- and *p*-type Si.^{3–11} Two peaks E40 and E150 were located at about $E_C - 0.09$ eV and $E_C - 0.28$ eV in the upper part of the band gap, whereas one peak H180 was detected in the lower band gap of Si. These peaks were previously attributed to different charge states (the single acceptor, the single donor, and the double donor) of interstitial Ti.^{3–5}

Usually, a charged defect upon emission an electron in *n*-type or a hole in *p*-type Si should exhibit the Poole-Frenkel effect, which describes the enhancement of the emission rate of the defect by electric field applied to the diode.¹² The electrical properties of a neutral defect remain insensitive to the variation of the electric field, except in the case of very high fields where tunneling processes could occur. In Ref. 5, the enhancement of the emission rate of E150 obtained from the shift of the conventional DLTS peak was shown to be significantly smaller than that expected for a charged defect in the frame of the Poole-Frenkel model. This inconsistency could be recently explained in Refs. 6 and 7 where we reported high-resolution Laplace DLTS spectra recorded at about 150 K in *n*-type Si hydrogenated by wet chemical etching in CP4A (27% HF + 46% HNO₃ + 27%

CH₃COOH) or CP6 (33.3% HF + 66.7% HNO₃) solution. In the hydrogenated Si samples, two other defects labelled E170 and E170' with similar electrical properties to E150 were observed. These peaks found only close to the surface could not be resolved from E150 by the conventional DLTS technique. Both E170 and E170' exhibit the enhancement of the emission rates as a function of electric field, which were previously interpreted as a weak shift of the conventional DLTS level E150. By using the high resolution Laplace DLTS technique, the emission rate of E150 was found to be almost constant up to 10⁶ V/m. This observation is not consistent with the attribution of this peak to the single donor state. Furthermore, an enhancement of the emission rate of E40 previously ascribed to the single acceptor was reported in Refs. 6, 7, and 13. The enhancement was shown to be in good agreement with the Poole-Frenkel model for a donor level in *n*-type Si.¹⁴

From *ab initio* molecular-dynamics simulations, the acceptor level of interstitial Ti was predicted to be buried in the conduction band, whereas the donor and double donor levels should be located at about $E_C - 0.76$ eV and $E_V + 0.15$ eV in the band gap of Si.¹⁵ Besides interstitial species substitutional Ti was also shown to introduce two electrically active levels: the single acceptor level close to the conduction band and the single donor level close to the valence band. The co-existence of substitutional and interstitial Ti was recently confirmed by Rutherford backscattering spectroscopy (RBS) and channeling-RBS measurements in Ti-implanted *n*-type Si.^{9,10} Two Ti-related defects were also detected by temperature dependent lifetime spectroscopy using photoluminescence and injection dependent photoconductance.¹⁰ The activation energy of the first trap was found to be similar to E150 while the second level was observed deeper in the band gap at around $E_C - 0.49$ eV, and it could

^{a)}Author to whom correspondence should be addressed. Electronic mail: kolkov@ifpan.edu.pl

not be attributed to any of deep Ti-related levels observed using by the DLTS measurements.

Recently, Markevich *et al.*¹⁶ studied float-zone (FZ) Si after implantation with Ti ions and subsequent annealing at 650 or 800 °C. By comparing secondary ion mass spectroscopy and DLTS depth profiles electrically active substitutional Ti species were excluded to appear in Si. The three dominant DLTS peaks observed in that study were attributed to the single acceptor, the single donor, and the double donor of interstitial Ti. One should notice that the Ti-related defects observed in Ref. 16 were shown to anneal out already at 650 °C, whereas higher annealing temperatures (around 900–1100 °C) were reported for the double donor Ti-related defect (H180) in *p*-type Si.¹¹ The discrepancy in annealing temperatures could be a result of the modification of the nearest neighborhood of the Ti-related defects by the implantation with heavy ions.

In Refs. 17–19, we showed that the use of the conventional DLTS technique alone could lead to the wrong interpretation of the experimental results, since defects with similar electrical properties cannot be properly resolved.

In the present study, we discuss the question as to the origin and the charge state of the dominant Ti-related defects in *n*- and *p*-type Si. In order to avoid radiation damage and inhomogeneous Ti profiles, we will use samples with a Ti doping in the melt. The TiH-complexes will be removed by annealing our samples at about 300–350 °C as reported in Ref. 4. DLTS, Laplace DLTS, and minority carrier transient spectroscopy (MCTS) measurements will be employed in order to shed light on the origin of the observed Ti defects. In addition, various heat treatments specified below will be used to compare the annealing behavior of the defects.

EXPERIMENTAL PROCEDURE

Samples were cut from Ti melt doped single crystalline silicon grown by the Czochralski (CZ) or by the FZ technique. Phosphorus was used for *n*-type and boron for *p*-type doping. The shallow doping concentrations were $\sim 7 \times 10^{14} \text{ cm}^{-3}$ (FZ) and $2 \times 10^{15} \text{ cm}^{-3}$ (CZ) in *n*-type Si, whereas these values were about $\sim 1 \times 10^{14} \text{ cm}^{-3}$ (FZ) and 7×10^{14} (CZ) in *p*-type Si. Before contact evaporation, the samples were annealed at about 300–350 °C in air or argon atmosphere in order to avoid H-related defects. Schottky contacts with the area of 5.3 mm² were formed by evaporation of aluminum for *p*-type and gold for *n*-type samples through a metal mask at room temperature. An eutectic InGa alloy is rubbed onto the back side of the samples to form the Ohmic contact. Before the evaporation of the Schottky contacts, samples were etched in a 1:2 mixture of HF and HNO₃ for approximately 5 s at room temperature to remove silicon dioxide from the surface of Si. The quality of the contacts was checked by current-voltage measurements at 45 K and at room temperature. In order to check the stability of the Ti-related defects, the samples were subjected to different annealing steps at temperatures in the range of 600–950 °C for 30–180 min in argon atmosphere. The shallow dopant profiles were determined by capacitance-voltage (C-V) measurements performed at 1 MHz. DLTS, MCTS, and

high-resolution Laplace DLTS measurements were used to investigate the electrical properties of deep defects in the band gap. The peak labeling used corresponds to that reported in Ref. 4. During MCTS measurements electron-hole pairs were generated by light illumination from the backside of our samples. The source of the illumination was an IR laser diode with a wavelength of 780 nm and the power of 70 mW. For the field effect measurements, the bias of the two filling pulses was kept constant (0 V and –1 V), whereas the reverse bias was varied from –10 V to –2 V. C-V measurements were used to determine the electric field in the depletion layer as described in Ref. 20.

EXPERIMENTAL RESULTS

Figure 1 shows conventional DLTS spectra (black symbols) recorded in Ti-doped *p*-type and *n*-type Si. Two dominant peaks labeled E40 and E150 were observed at around 40 K and 150 K in *n*-type Si, and one peak labeled H180 was detected at about 180 K in *p*-type Si. These peaks were observed in both FZ and CZ grown Si irrespective on the doping level of the samples, and they become the main point of interest in the present study. In order to confirm the presence of the dominant peaks, E40 and E150 in *p*-type Si MCTS measurements were performed. During the MCTS measurements, the optical excitation instead of electrical filling pulses is used. This allows us to detect electrically active deep levels located in the upper half of the band gap in *p*-type Si. The MCTS spectrum (gray symbols) recorded in *p*-type Si is presented in Fig. 1, and it shows that indeed both E40 and E150 also exist in *p*-type Si. In order to analyze the electrical properties of the peaks presented in Fig. 1, the high resolution Laplace DLTS technique was employed.

Figure 2 shows Laplace DLTS spectra recorded at 45 K and 165 K in Ti-doped *n*-type Si. In good agreement with the DLTS spectra of Fig. 1, two dominant Laplace DLTS peaks E40 and E150 were observed at 45 K and 165 K, respectively. Also one dominant peak was observed at 180 K in *p*-type Si (the inset in Fig. 2). From the Arrhenius plots of

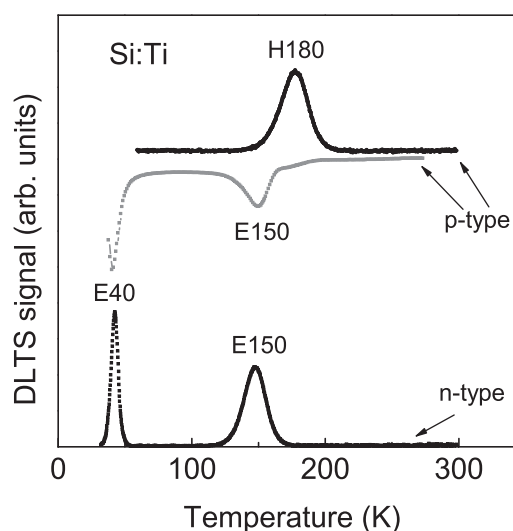


FIG. 1. Conventional DLTS (black symbols) and MCTS (grey symbols) spectra recorded in FZ Si annealed at 350 °C.

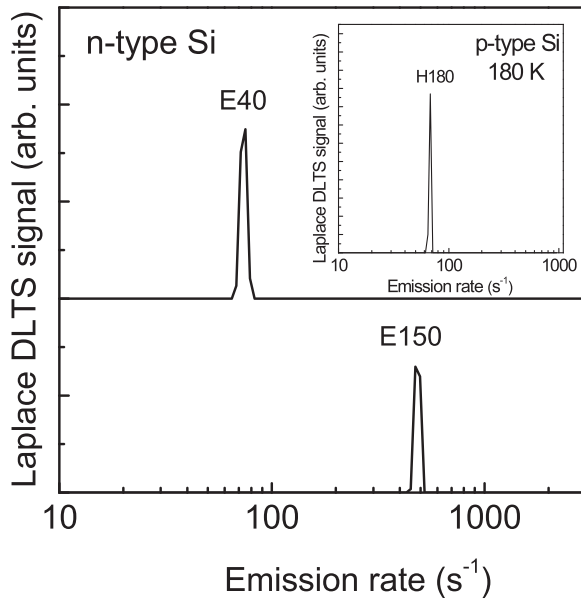


FIG. 2. Laplace DLTS spectra recorded at 45 K and 165 K in *n*-type Si. The inset shows a Laplace DLTS spectrum observed at 180 K in *p*-type Si.

T^2 -corrected electron emission rates derived from Laplace DLTS measurements (Fig. 3), we determined the electrical properties of the defects corresponding to E40, E150, and H180 (see Table I). One should notice that the activation enthalpy and the apparent capture cross section of the defects are slightly different from those previously reported in Refs. 3–5 and 8. However, the determination the electrical properties of the traps observed by high-resolution Laplace DLTS in annealed samples leads to more precise values compared to those obtained previously by the conventional DLTS measurements.

As mentioned above, the Poole-Frenkel effect is often used to differentiate between donor-like and acceptor-like character of deep levels in semiconductors. The thermal emission of a charge carrier from a localized electronic state is enhanced in an electric field E through a lowering of the potential energy barrier. Therefore, a charged defect upon

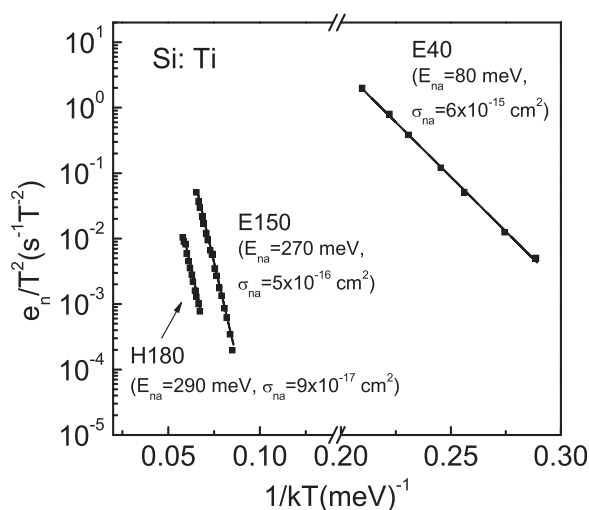


FIG. 3. Arrhenius plots recorded for the traps observed in Figs. 1 and 2.

TABLE I. The electrical fingerprints (the activation enthalpy and the apparent capture cross section) and concentrations (after annealing at 300 °C) of the defects observed in Fig. 1.

Defects	E40	E150	H80
Activation enthalpy (meV)	80	270	290
Apparent capture cross section (cm ²)	6×10^{-15}	5×10^{-16}	9×10^{-17}
Concentration (cm ⁻³)	9×10^{13}	9×10^{13}	5×10^{13}

emission of an electron (hole) is expected to display the Poole-Frenkel effect. In contrast, defects in neutral charge state upon carrier emission are not affected by an applied field. Following this idea, we investigate the emission rates of E40, E150, and H180 as a function of electric field in *n*- and *p*-type Si. Fig. 4 shows high-resolution Laplace DLTS spectra recorded with different reverse biases at 45 K (dashed line) and 165 K (solid line). E40 shifts towards the higher emission rates with the higher bias applied to the diode, whereas no changes of the emission rate were observed for E150. In order to quantitatively describe the enhancement of the emission rate of E40, the field dependences derived in Ref. 14 were applied.

Figure 5 shows the emission rate of E40 as a function of the square root of the electric field. The experimental points were found to be in good agreement with the results of calculations (solid line in Fig. 5) performed in the frame of the Poole-Frenkel model¹⁴ for electric field below 2×10^6 V/m. The slope of the fitting curve was described as $(e^3/\pi\epsilon\epsilon_0)^{1/2}/kT$, where e is the elementary charge, ϵ is the dielectric constant, and ϵ_0 is the vacuum permittivity. We notice that the enhancement of the emission rate of E40 becomes faster compared to the theory at the higher values of the electric field. The experimental points above 2×10^6 V/m can be well described by the straight line in the inset of Fig. 5, where the emission rate of E40 is plotted versus the square of the electric field. The electric field above 2×10^6 V/m is high enough that phonon-assisted tunneling becomes dominant in our samples. In this case, Ganichev *et al.*¹⁴ calculated an emission

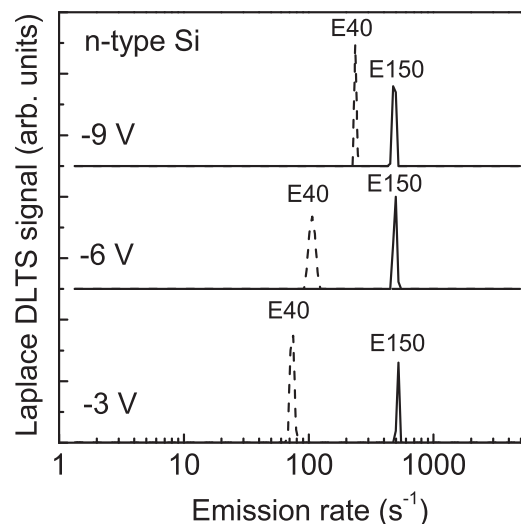


FIG. 4. Laplace DLTS spectra recorded at 45 K and 165 K at different bias in FZ *n*-type Si.

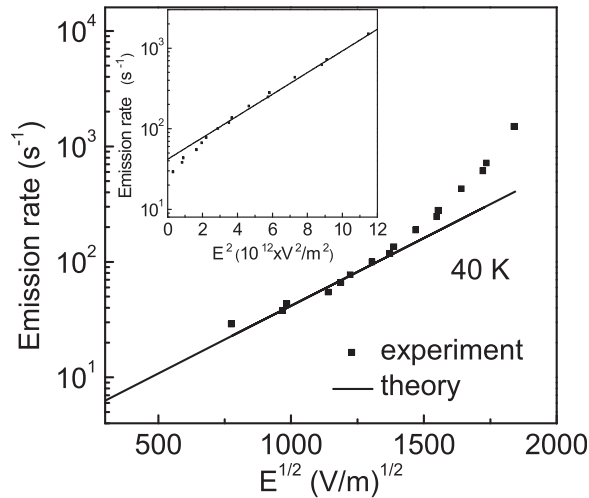


FIG. 5. Field dependence of the emission rate of E40 is compared to the Poole-Frenkel model (solid line). The inset shows changes of the electron-emission rate of E40 as a function of the square of the electric field where the solid line is the fitting of the experimental data lying above $4 \times 10^{12} \text{ V}^2/\text{m}^2$.

rate proportional to $\exp(E^2/E_C^2)$, where E_C was a characteristic field strength.

Figure 6 shows the changes of the emission rate as a function of the square root of the electric field observed for H180 in *p*-type Si. In good agreement with the results of Refs. 6 and 7, the emission rate of H180 was found to be almost constant in the whole range of the electric field.

Figure 7 shows the depth profile of E40, E150, and H180 in *FZ* grown Si annealed at 300°C . We notice that the concentration of E40 and E150 was found to be identical in this sample. This result is contradictory to those presented in Ref. 13. However, the depth profiles obtained at temperatures close to a “freeze-out” temperature (around 40 K in *n*-type Si) should be taken with care since the increase of the series resistance could lead to the wrongly determined capacitance of the diode. In order to avoid the effect of the series resistance, we recorded the depth profiles of E40 at a higher temperature (45 K) compared to that used in Ref. 13. An equal concentration of E40 and E150 was also obtained in *CZ* Si annealed at 300°C . Similarly to E40 and E150, the concentration of H180 was

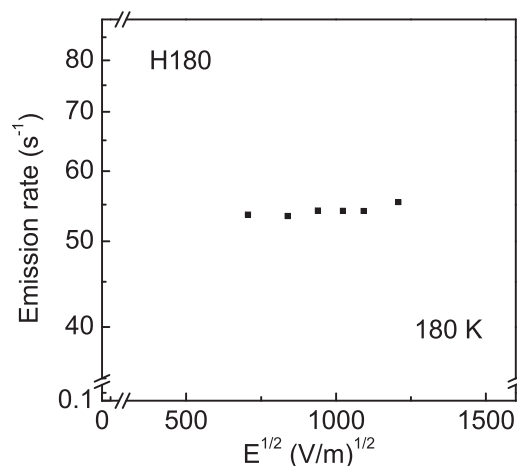


FIG. 6. The emission rate versus the square root of the electric field plotted for H180.

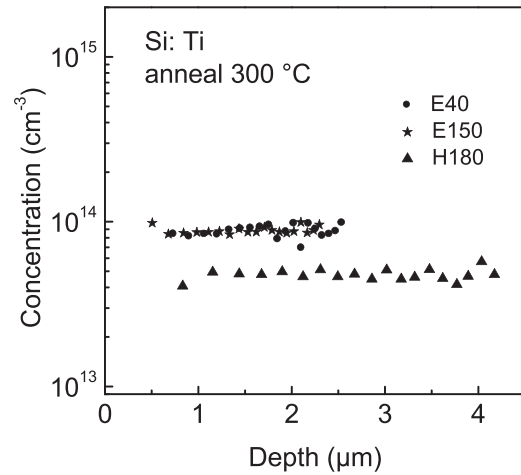


FIG. 7. Concentration depth profiles of E40, E150, and H180 recorded in *n*-type Si annealed at 300°C .

found to be also constant in *p*-type Si. The lower concentration of H180 (around $5 \times 10^{13} \text{ cm}^{-3}$) compared to those obtained for E40 and E150 can be interpreted by different growth conditions of the *p*- and *n*-type samples.

In order to check the thermal stability of the defects corresponding to the peaks observed in *n*- and *p*-type Si, we anneal some of our samples in the range of 600°C – 850°C in argon atmosphere. After the heat treatment, the samples were quenched. The amplitude of the dominant peaks E40, E150, and H180 was constant after annealing below 850°C and it decreases at higher temperatures. Fig. 8 shows the depth profiles of E40 and E150 recorded in *n*-type samples annealed at 850°C for 60 min (grey lines). The concentration of these defects in the annealed samples was reduced by a factor of 4 compared to that detected before the annealing. One should also notice that even after the heat treatment both E40 and E150 exhibit almost identical depth profiles. The concentration of H180 was also significantly reduced after the annealing at above 850°C (not shown here), and it is consistent with the findings previously reported in Ref. 11.

If *n*-type Si samples doped with Ti are subjected to hydrogenation by wet chemical etching or a H plasma

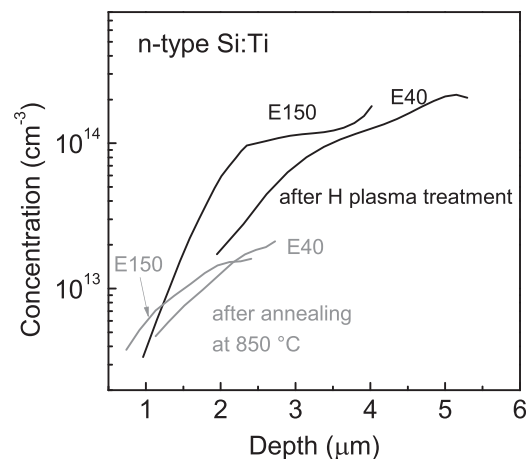


FIG. 8. Concentration depth profiles of E40 and E150 recorded in *n*-type Si annealed at 850°C (black lines) and after hydrogenation by H plasma treatment (grey lines).

treatment the concentration of E40 and E150 decreases differently towards the surface (black lines in Fig. 8). We notice that the shift of the profiles is above all possible uncertainties. These findings are similar to those previously reported in Refs. 4 and 6. It is well-known that in hydrogenated samples H could easily react with the Ti-related defects leading to the formation of electrically active TiH-related complexes, which are stable up to 100 °C.^{4,6} The higher concentration of the TiH-defects close to the surface results in the decrease of E40 and E150 in this region. Different concentrations of E40 and E150 close to the surface suggest that these peaks belong to different Ti-related defects.

DISCUSSION

The results of the present study are not consistent with the assignments of E40, E150, and H180 to different charge states of interstitial Ti. The Poole-Frenkel effect observed for E40 below 2×10^6 V/m shows unambiguously that the defect is the single donor. The absence of the field-effect for E150 attributes the defect to the single acceptor. Mathiot and Hocine⁵ argued that the absence of the enhancement of E150 with electric field could be correlated with thermally activated capture of electrons with an energy barrier of about 20 meV. However, we notice that this value is comparable with the thermal energy ($3kT/2$) at 150 K. Since the capture of free electrons is a multi-phonon process, the absence of the enhancement of the emission rate of E150 cannot be properly explained only by the presence of the barrier which should be transparent for electrons at such temperatures.

One should also emphasize that the capture cross-section of E40 (around 3×10^{-14} cm²) was found to be about 10 times larger than that of E150. It is well-established in Si that the capture cross section is expected to be about 10^{-14} cm² for Coulombically attractive centers, whereas one expects this value to be in the range 10^{-16} – 10^{-15} cm² for a neutral defect and less than 10^{-17} cm² for a repulsive defect.¹⁷ Then the larger capture cross section of E40 in comparison to E150 is also consistent with the attribution of these defects to the single donor and the single acceptor, respectively.

Furthermore, different depth profiles obtained close to the surface in samples subjected to hydrogenation may also suggest that E40 and E150 do belong to a single donor and a single acceptor of different origin, respectively. Isolated H is known to be negatively charged in *n*-type Si.^{21,22} Then, a stronger decrease of E40 towards the surface in comparison to E150 can be explained by more efficient interaction of positively charged E40 with negatively charged H instead of neutral E150 at room temperature.

The previous assignment of H180 to the double donor state can be consistent with the weak enhancement of the emission rate of this defect under electric field (see Fig. 6). The total potential of a double-donor defect in *p*-type Si should consist of an attractive potential in the centre and a repulsive potential outside the centre. The attractive potential is usually weaker than an attractive Coulombic potential, and this could result in the reduction of the enhancement of the emission rate of the defect in comparison to that predicted in

the frame of the Poole-Frenkel model. Similarly, the double donor state of Pt shows a weaker electric field dependence of the emission rate in *p*-type Si.²³ Besides this thermally activated capture of holes with a barrier of about 40 meV was reported for H180 in Ref. 24. In support of this idea, Buchwald and Johnson²⁵ reported that the absence of the enhancement of the emission rate of EL2 assigned to the single donor state in *n*-type GaAs could be correlated with thermally activated capture of electrons with an energy barrier of 40 meV.

According to the *ab-initio* calculations, the interstitial Ti should have a positive-*U* sequence of the levels in the bandgap of Si where only two donor levels of interstitial Ti should be located in the band gap, whereas the single acceptor level should be resonant with the conduction band.¹⁵ The positive-*U* system means that the second carrier on the defect should be the more loosely bound than the first one, and the acceptor level should be located closer to the conduction band than the donor level. Therefore, the presence of the Poole-Frenkel effect for E40 and its absence for E150 is contradictory to the previous assignment of E40 and E150 to the same defect (interstitial Ti), since here the order of acceptor and donor levels is reversed.

In contrast, equal concentrations of E40 and E150 were observed in bulk of Si in as-grown samples, and those subjected to H plasma treatments or different annealing steps at 300 °C, 600 °C, and 850 °C. Identical concentrations of these defects have been also reported in Ref. 16, whereas different concentrations of E40 and E150 were observed in Ref. 4. Until now, we cannot explain the identical depth profiles of E40 and E150 in bulk of Si. However, the equal concentrations of defects as obtained from DLTS measurements are certainly a necessary condition but it is not sufficient in order to assign them to different charge states of the same defect. Previously, based on equal concentrations of the levels as obtained from Hall-effect measurements,^{26,27} substitutional gold was believed to introduce two levels in the band gap of Si.²⁸ In contrast, Lang *et al.*²⁹ showed that in some samples the concentration obtained from the height of the donor DLTS peak was significantly lower compared to that from the single acceptor level. Similarly, Cu was considered as a deep defect introducing three levels in the band gap of GaAs.²⁸ This conclusion has been drawn from equal concentrations as obtained from Hall-effect measurements. Afterwards, however, photoluminescence measurements showed different symmetry of two levels,³⁰ and therefore they could not be attributed to the same defect.

We also notice that only the presence of the positive charged state of interstitial Ti was confirmed by the electron paramagnetic resonance studies³¹ which, in contrast to DLTS measurements, could directly determine the structure of the defect.

Wang and Sah³ reported that two independent levels from two different defects could not give the same recombination characteristics as two levels, which belong to different charge states of the same defect. From their electrical measurements, only H180 could be attributed to the double donor, whereas no evidences have been found that E150 and H180 belonged to the same defect.

In addition, the emission of an electron from E40 and E150 to the conduction band leads to very different entropy changes of $2k$ and $-4k$, respectively, whereas these changes were around $0.5k$ for H180 in p -type Si.³² The negative changes of entropy of E150 could not be explained in Ref. 32, and the authors could not conclude if E150 indeed belonged to the interstitial Ti defect.

As mentioned above, according to the *ab-initio* calculations, the single acceptor state and the single donor state of substitutional Ti should be electrically active in n -type Si.¹⁵ The uncertainty of the theory in the determination the energy level position of defects may result in the shift of these levels in the band gap. In this case, the single acceptor could correspond to E150, whereas the single donor state of substitutional Ti might be located close to the valence band or even buried into the valence band and, therefore, it could not be detected by DLTS measurements. However, no direct evidences have been found for this assignment. In contrast, Lemke und Zulehner³³ suggested that only interstitial Ti defects could be formed during the growth of Si, whereas substitutional Ti appeared after interaction of Ti_i with vacancies by the cooling down the samples below a critical temperature. According to Ref. 15, the reaction of $Ti_i + V \rightarrow Ti_S$ should occur with a large energy gain of about 2.7 eV and, therefore, the presence of equal concentrations of Ti_i and Ti_S could be improbable in a sample doped with Ti during the growth.

The presence of interstitial and substitutional Ti is also contradictory to the findings of Ref. 34 where the free carrier concentration was found to increase from $2.2 \times 10^{13} \text{ cm}^{-3}$ to about 10^{17} cm^{-3} in samples subjected to a Ti implantation with a dose of 10^{15} cm^{-2} . These observations were correlated with additional Ti donors induced by the implantation and assigned to E150. However, besides electrically active Ti-related defects high concentrations of vacancy- and/or interstitial-related complexes could be also created by high-energy implantation of Ti with relatively high doses in n -type Si. This makes the interpretation of the results presented in Ref. 34 ambiguous. Supporting this idea, the annealing temperature of the Ti-related defects created by high energy ion implantation¹⁶ is significantly lower compared to the samples with Ti introduced directly during the growth process.

Summarizing, the observed results cannot be explained in the frame of the model where three levels (E40, E150, and H180) belong to the same defect (presumably interstitial Ti) as suggested in Refs. 3–5 or by the model where E40 and H180 belong to different charge states of interstitial Ti and E150 is the acceptor state of substitutional Ti as suggested in Refs. 6 and 7. We suggest that some theoretical calculations could be helpful in order to resolve this puzzle.

CONCLUSIONS

We presented a combining DLTS, high-resolution Laplace DLTS, and MCTS measurement study on Ti-doped Si samples. We questioned the assignment of three dominant DLTS peaks (E40, E150, and H180) observed in n - and p -type Ti-doped Si to the single acceptor, the single donor, and

the double donor of interstitial Ti. The activation enthalpy of the defects obtained from Laplace DLTS measurements was found as 80 meV (E40), 270 meV (E150), and 290 meV (H180), and their apparent capture cross section was characterized by $6 \times 10^{-15} \text{ cm}^2$, $5 \times 10^{-16} \text{ cm}^2$, and $9 \times 10^{-17} \text{ cm}^2$, respectively. These values were found to be more precise in comparison to those obtained previously by conventional DLTS measurements in samples subjected to hydrogenation. We showed that the emission rate of E40 was significantly enhanced with electric field. In the electric field region below $2 \times 10^6 \text{ V/m}$, the enhancement could be well explained by the Poole-Frenkel effect, which usually appeared for defects with the attractive Coulombic potential. At higher electric fields, the phonon-assisted tunneling became dominant. The emission rate of E150 was found to be constant in the whole range of electric fields. These results were not consistent with the previous assignment of these levels to different charge states of interstitial Ti. The attribution of H180 to the double donor was in good agreement with the results of the present investigation. However, we could not explain the identical depth profiles observed in bulk Si in as-grown, hydrogenated, and annealed samples.

¹J. T. Borenstein, J. I. Hanoka, B. R. Bathey, J. P. Kalejs, and S. Mil'shtein, *Appl. Phys. Lett.* **62**, 1615 (1993).

²G. Coletti, P. C. P. Bronsveld, G. Hahn, W. Warta, D. Macdonald, B. Ceccaroli, K. Wambach, N. Le Quang, and J. M. Fernandez, *Adv. Funct. Mater.* **21**, 879 (2011).

³A. C. Wang and C. T. Sah, *J. Appl. Phys.* **56**, 1021 (1984).

⁴W. Jost and J. Weber, *Phys. Rev. B* **54**, R11038 (1996).

⁵D. Mathiot and S. Hocine, *J. Appl. Phys.* **66**, 5862 (1989).

⁶Vi. Kolkovsky, L. Scheffler, and J. Weber, *Physica B* **439**, 24 (2014).

⁷Vi. Kolkovsky, L. Scheffler, and J. Weber, *Phys. Status Solidi C* **9**, 1996 (2012).

⁸J.-W. Chen, A. G. Milnes, and A. Rohatgi, *Solid-State Electron.* **22**, 801 (1979).

⁹J. R. Morante, J. E. Carceller, and P. Cartujo, *Solid-State Electron.* **26**, 1 (1983).

¹⁰T. Roth, M. Rüdiger, W. Warta, and S. W. Glunz, *J. Appl. Phys.* **104**, 074510 (2008).

¹¹S. Hocine and D. Mathiot, *Appl. Phys. Lett.* **53**, 1269 (1988).

¹²J. L. Hartke, *J. Appl. Phys.* **39**, 4871 (1968).

¹³J. Weber, L. Scheffler, V. Kolkovsky, and N. Yarykin, *Solid State Phenom.* **205–206**, 245 (2014).

¹⁴S. D. Ganichev, E. Ziemann, W. Prettl, I. N. Yassievich, A. A. Istratov, and E. R. Weber, *Phys. Rev. B* **61**, 10361 (2000).

¹⁵D. J. Backlund and S. K. Estreicher, *Phys. Rev. B* **82**, 155208 (2010).

¹⁶V. P. Markevich, S. Leonard, A. R. Peaker, B. Hamilton, A. G. Marinopoulos, and J. Coutinho, *Appl. Phys. Lett.* **104**, 152105 (2014).

¹⁷L. Scheffler, Vi. Kolkovsky, and J. Weber, *J. Appl. Phys.* **113**, 183714 (2013).

¹⁸L. Scheffler, Vi. Kolkovsky, and J. Weber, *J. Appl. Phys.* **116**, 173704 (2014).

¹⁹Vi. Kolkovsky, A. Mesli, L. Dobaczewski, N. V. Abrosimov, Z. R. Zytikiewicz, and A. R. Peaker, *Phys. Rev. B* **74**, 195204 (2006).

²⁰P. Blood and J. W. Orton, *The Electrical Characterization of Semiconductors: Majority Carriers and Electron States* (Academic Press, USA, 1992).

²¹C. G. Van de Walle, P. J. H. Denteneer, Y. Bar-Yam, and S. T. Pantelides, *Phys. Rev. B* **39**, 10791 (1989).

²²K. B. Nielsen, B. B. Nielsen, J. Hansen, E. Andersen, and J. U. Andersen, *Phys. Rev. B* **60**, 1716 (1999).

²³H. Zimmermann and H. Ryssela, *Appl. Phys. Lett.* **58**, 499 (1991).

²⁴S. Kuge and H. Nakashima, *Jpn. J. Appl. Phys., Part 1* **30**, 2659 (1991).

²⁵W. R. Buchwald and N. M. Johnson, *J. Appl. Phys.* **64**, 958 (1988).

²⁶C. Collins, R. O. Carlson, and C. J. Gallagher, *Phys. Rev.* **105**, 1168 (1957).

²⁷G. Bemski, *Phys. Rev.* **111**, 1515 (1958).

²⁸G. Milnes, *Deep Impurities in Semiconductors* (Wiley, New York, 1973).

- ²⁹D. V. Lang, H. G. Grimmeiss, E. Meijer, and M. Jaros, [Phys. Rev. B](#) **22**, 3917 (1980).
- ³⁰F. Willmann, D. Bimberg, and M. Blatte, [Phys. Rev. B](#) **7**, 2473 (1973).
- ³¹D. A. van Wezep, R. van Kemp, E. G. Sieverts, and C. A. J. Ammerlaan, [Phys. Rev. B](#) **32**, 7129 (1985).
- ³²L. Tilly, H. G. Grimmeiss, H. Petersson, K. Schmalz, K. Tittelbach, and H. Kerkow, [Phys. Rev. B](#) **43**, 9171 (1991).
- ³³H. Lemke and W. Zulehner, [Physica B](#) **273**, 398 (1999).
- ³⁴J. Olea, M. Toledano-Luque, D. Pastor, G. Gonzalez-Diaz, and I. Martil, [J. Appl. Phys.](#) **104**, 016105 (2008).